A Compact and Low Profile Loop Antenna with Six Resonant Modes for LTE Smartphone

Hang Xu, HanYang Wang, Steven Gao, Hai Zhou, Yi Huang, Qian Xu and YuJian Cheng

***Abstract*—In this paper, a novel six-mode loop antenna covering 660-1100 MHz, 1710-3020 MHz, 3370-3900 MHz, and 5150-5850 MHz has been proposed for the application of Long Term Evolution (LTE) including the coming LTE in unlicensed spectrum (LTE-U) and LTE-Licensed Assisted Access (LTE-LAA). Loop antennas offer better user experience than conventional Planar Inverted-F Antennas (PIFA), Inverted-F Antennas (IFA), and monopole antennas because of their unique balanced modes (1λ, 2λ, …). However, the bandwidth of loop antennas is usually narrower than that of PIFA/IFA and monopole antennas due to these balanced modes. To overcome this problem, a novel monopole/dipole parasitic element, which operates at an unbalanced monopole-like 0.25λ mode and a balanced dipole-like 0.5λ mode, is first proposed for loop antennas to cover more frequency bands. Benefiting from the balanced mode, the proposed parasitic element is promising to provide better user experience than conventional parasitic elements. To the authors' knowledge, the balanced mode for a parasitic element is reported for the first time. The proposed antenna is able to provide excellent user experience while solving the problem of limited bandwidth in loop antennas. To validate the concept, one prototype antenna with the size of 75×10×5 mm^3 is designed, fabricated and measured. Both simulations and experimental results are presented and discussed. Good performance is achieved.**

***Index Terms*—Loop antennas, handset antennas, mobile antennas, multi-band antenna, LTE antenna, LTE-Unlicensed (LTE-U), LTE-Licensed Assisted Access (LTE-LAA),parasitic element.**

I. Introduction

ULTRA-THIN smartphones have become essential devices in people's daily life due to their powerful functionality such as navigation, entertainment, social networking service, mobile financial service, and so on. Loop antennas have received extensive attention for Long Term Evolution (LTE) smartphones due to their unique features such as multimode and balanced modes (1λ, 2λ,…) [1]-[12]. The balanced modes have much weaker surface current distribution on printed circuit board (PCB) than the unbalanced modes which are the common operating modes of Planar Inverted-F Antennas (PIFA), Inverted-F Antennas (IFA), and monopole antennas [13]-[18]. This property can give loop antennas better user interaction robustness and smaller antenna performance degradation than conventional PIFA/IFA and monopole antennas when a mobile phone is held by a user's hand or attached to a user's head [19]-[21]. This is important for user experience in smartphone application.

However, weaker surface current distribution on PCB also means less effective radiation area for loop antennas. As a result, the bandwidth of loop antennas is usually narrower than that of conventional PIFA/IFA and monopole antennas. To overcome the problem of limited bandwidth, there has been lots of research work on loop antennas for mobile phones. Nevertheless, the loop antennas in [1], [5], and [20] can excite only three resonant modes including 0.5λ, 1λ, and 1.5λ modes, which limits their bandwidth. In [11] and [12], reconfigurable technology was applied in loop antenna but the covered bandwidth is still limited. Recently, the fourth mode, i.e. 2λ mode, was reported in [4] and [7] to cover wider frequency band (698-960 MHz and 1710-2300 MHz in [4]; 800-1100 MHz and 1700-2580 MHz in [7]), but the bandwidth is still not wide enough for LTE application and even the coming LTE in unlicensed spectrum (LTE-U) and LTE-Licensed Assisted Access (LTE-LAA) application [22]-[23]. Therefore, although many scientists have made a lot of effort, it is still a tremendous challenge for loop antennas to enjoy the excellent user experience while obtaining a bandwidth wide enough for LTE smartphone application.

In this paper, a novel six-mode loop antenna covering 660-1100 MHz, 1710-3020 MHz, 3370-3900 MHz, and 5150-5850 MHz is proposed for LTE smartphones. The bandwidth of the proposed antenna is wide enough for almost all the service of mobile telecommunication systems, namely GSM/UMTS/LTE, including LTE bands 42/43 (3400-3800 MHz) and LTE-U/LTE-LAA (5150-5850 MHz) as well. The distinctive feature of the proposed antenna is that not only four loop antenna modes, i.e. 0.5λ, 1λ, 1.5λ, and 2λ modes have been excited, but also two extra modes are generated by a proposed monopole/dipole parasitic element, i.e. an unbalanced monopole-like 0.25λ mode and a balanced dipole-like 0.5λ mode. Usually, a parasitic element operates at an unbalanced monopole-like 0.25λ mode and/or an unbalanced 0.75λ mode

This work is funded by Huawei Technology Ltd, China.

H. Xu and S. Gao are with the School of Engineering and Digital Arts, University of Kent, Canterbury, CT2 7NT, United Kingdom (e-mail: S.Gao@kent.ac.uk and Hx21@kent.ac.uk).

H.Y. Wang and H. Zhou are with Huawei Technology Ltd, 300 South Oak Way, Green Park, Reading RG2 6UF, Berkshire, United Kingdom (e-mail: Hanyang.Wang@huawei.com and Hai.Zhou1@huawei.com).

Y. Huang and Q. Xu are with the Department of Electrical Engineering and Electronics, University of Liverpool, Liverpool, L69 3GJ United Kingdom .

Y.J. Cheng is with the EHF Key Laboratory of Fundamental Science, School of Electronic Engineering, University of Electronic Science and Technology of China (UESTC), Chengdu 611731, China

but not a balanced dipole-like 0.5λ mode, so it should be the first time to report that a parasitic element could operate at a balanced dipole-like 0.5λ mode. Benefiting from the wideband feature and the three balanced modes, the proposed antenna is able to provide excellent user experience while solving the problem of limited bandwidth in loop antennas. The proposed antenna has been simulated, fabricated and measured. All the simulated results were obtained by using Ansoft HFSS [24]. The measured reflection coefficient and radiation efficiency were obtained by using a Rohde & Schwarz vector network analyzer and a reverberation chamber, respectively [25]-[27].

II. Methodology, Analysis and Discussions of Bandwidth Enhancement Technology

In order to explain the concept of the proposed antenna clearly, this section starts from the design of one four-mode loop antenna with enhanced bandwidth in Part A. In Part B, a single-mode parasitic element is introduced at first and then further developed to a monopole/dipole parasitic element to cover LTE bands 42/43 and LTE-U/LTE-LAA. In-depth analysis and discussions about radiation mechanisms are presented in Part C. In Part D, some design guidance is given.

A. Bandwidth Enhancement for Loop Antenna Modes

In this part, a four-mode loop antenna that can cover 680-1000 MHz and 1665-2765 MHz is proposed as a starting point.

1) Antenna Configuration

The configuration of the proposed four-mode loop antenna is shown in Fig. 1. It is designed on a single-sided PCB (Ɛr = 4.4, loss tangent = 0.02) with the dimension of 145×75×1.6 mm^3. The antenna is placed on a 5 mm high foam carrier (Ɛr = 1) which is located at the bottom edge of the PCB, as shown in Fig. 1(a). There is a 10 mm ground plane clearance below the antenna, so the total antenna volume is 75×10×5 mm^3.

The loop antenna has two connections to the PCB. One is a feeding point and the other is a grounding point as shown in Fig. 1(b) and (c). Most parts of the antenna have an identical width of 1 mm except two loading/de-loading parts [28]. In Fig. 1(c), detailed dimensions of the antenna are shown and the dashed line is for bending the antenna track. The coplanar waveguide (CPW) portion on the PCB is used for a matching circuit to enhance the bandwidth of 0.5λ mode.

2) Bandwidth Comparison and Analysis

Simulated S11 of the antenna in Fig. 1 is shown in Fig. 2. In low band, the -6 dB impedance bandwidth can cover 833-973 MHz, and then it can be further enhanced by a highpass matching circuit to cover 680-1000 MHz (the highpass matching circuit will be shown in Section IV). In high band, the -6 dB impedance bandwidth can cover 1665-2765 MHz, which is wider than the four-mode loop antennas in [4] (1710-2300 MHz) and [7] (1700-2580 MHz).

One important issue of the proposed design is the use of a widened portion A (shown in Fig. 1), which has significant effect on the bandwidth enhancement of 1λ, 1.5λ, and 2λ modes. In order to explain the principle of the bandwidth enhancement, vector current distribution of 1.5λ mode is plotted in Fig. 3 for three antennas including two reference antennas (Ref-1 and Ref-2) and the proposed loop antenna. Except the widened portion A, the rest parts of reference antennas are the same as the proposed antenna. From Fig. 3(a) and (b), it can be seen that there is only one current path along the antenna track. From Fig. 3(c), it is clearly shown that there are multi current paths in the widened portion A and different current paths have different electrical length, which means the combination of different current paths can have wider bandwidth. This is how the bandwidth is enhanced by the widened portion A.

To demonstrate our analysis, simulated S11 of the three antennas is shown in Fig. 4. As predicted, for the 1λ mode, the relative bandwidth increases from 7.2% (Ref-1) and 6.8% (Ref-2) to 10.4% (proposed antenna). For the 1.5λ mode, the relative bandwidth increases from 7.6% (Ref-1) and 8.6% (Ref-2) to 21.3% (proposed antenna). For the 2λ mode, the relative bandwidth increases from 12.8% (Ref-1) and 13.1% (Ref-2) to 17.5% (proposed antenna). As a result, the total relative bandwidth of 1λ, 1.5λ, and 2λ modes increases from 27.6% (Ref-1) and 28.5% (Ref-2) to 49.2% (proposed antenna) because of the widened portion A.

However, this bandwidth enhancement technique has little effect on the bandwidth of 0.5λ mode. The reason is that in the frequency range below 1 GHz, PCB contributes most of the radiation rather than the antenna [29], so the improvement of current path on antenna track has limited effect on the bandwidth.

B. Evolution of Parasitic Element Technology

According to the result in Part A, 680-1000 MHz and 1665-2765 MHz can be fully covered by using one loop antenna. Nevertheless, the bandwidth is still not wide enough to meet the requirement of mobile telecommunication service, but the bandwidth of four-mode loop antennas has come to the extremity. In this part, parasitic element technology is introduced and further developed to cover more frequency bands.

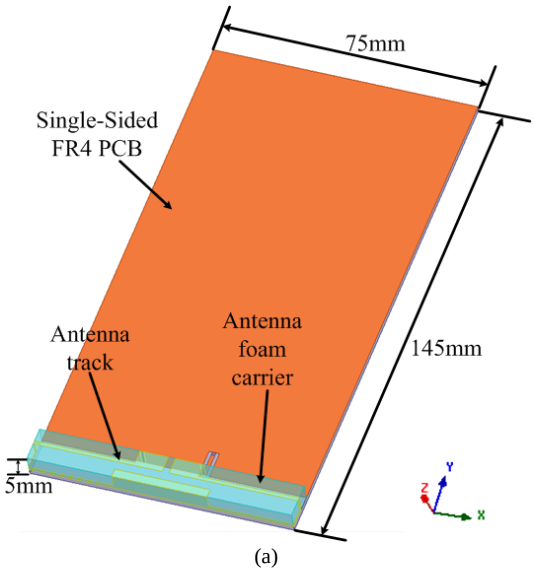

(a)

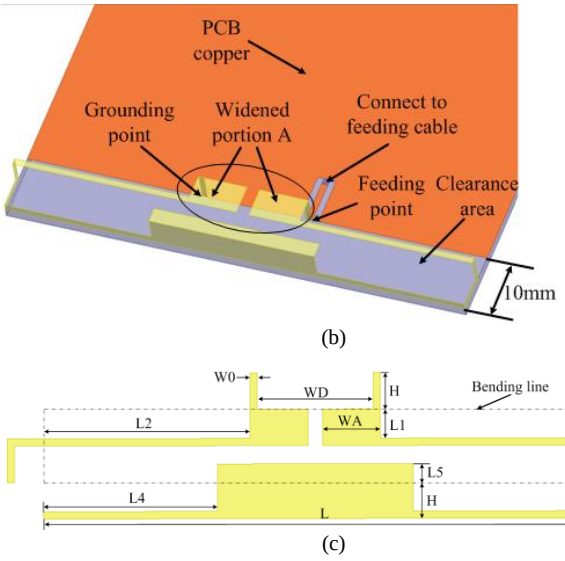

Fig.1.Geometryof a four-mode loop antenna. (a) Antenna with PCB. (b) Antenna track. (c) Dimension of antenna track. WD = 16, W0 = 1, H = 5, WA = 8, L1 = 4, L2 = 28.5, L3 = 5, L4 = 24 and L5 = 2.5 mm.

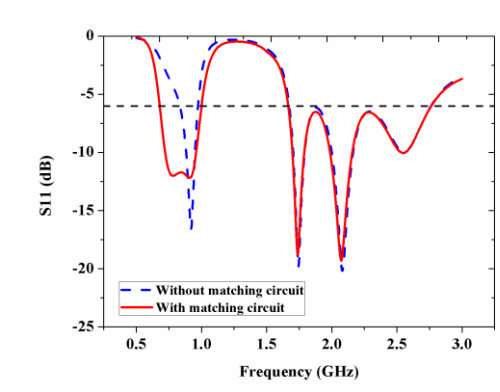

Fig. 2. Simulated S11 of the proposed four-mode loop antenna.

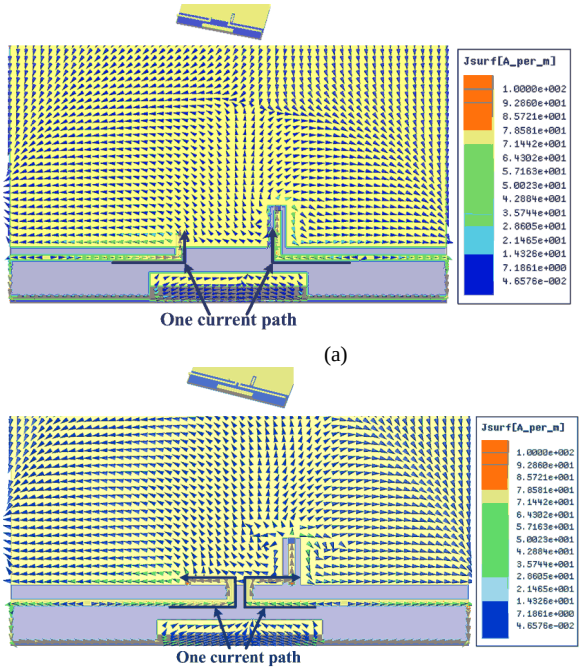

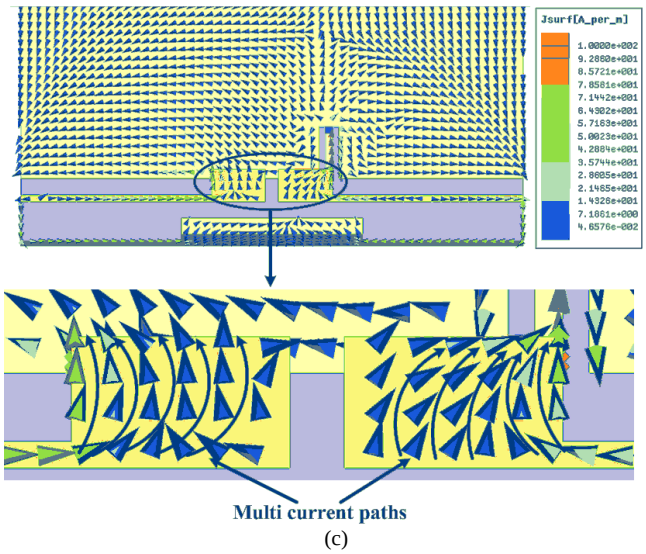

Fig. 3. Vector current distribution. (a) Ref-1. (b) Ref-2. (c) Proposed loop antenna.

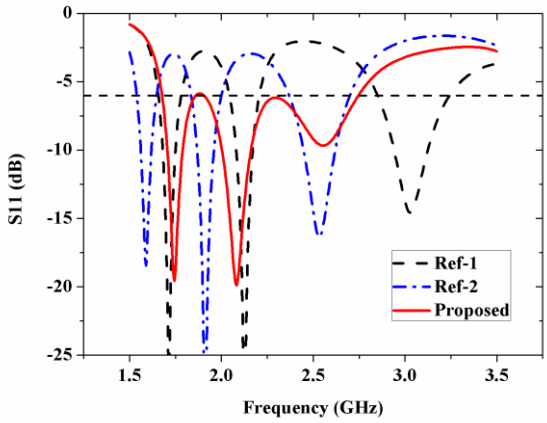

Fig. 4. Simulated S11of Ref-1, Ref-2 and proposed loop antennas.

1) Single-Mode Parasitic Element

At first, a single-mode parasitic element is introduced for loop antennas. Based on the loop antenna in Fig. 1, a grounding strip is placed near the feeding point as shown in Fig. 5(a). This parasitic element can create one mode to cover LTE Band 42 (3400-3600 MHz), which can be seen from Fig. 5(b).

However, this technique cannot be used to excite a mode in 5 GHz band for LTE-U/LTE-LAA through our simulation. In order to explain the reason, the vector current distribution at 5.5 GHz is shown in Fig. 5 (c) for LL = 8.5 mm. From Fig. 5(c), it can be observed that there are two anti-phase currents that simultaneously couple electromagnetic field energy from the main loop antenna to the single-mode parasitic element. Nevertheless, the coupling energy from the two anti-phase currents excites the same 0.25λ modes but with anti-phase, so the excited 0.25λ modes will cancel each other. As a result, the single-mode parasitic element cannot be excited efficiently in 5 GHz band.

2) Monopole/Dipole Parasitic Element

To solve the energy cancellation problem, an abstract current

path model is extracted from Fig. 5(c) and shown in Fig. 6(a). I_{loop1} and I_{loop2} are the corresponding anti-phase currents on the main loop antenna; I_{pe} is the excited mode current on the parasitic element; α is the coupling coefficient between I_{loop1} and I_{pe}, and β is the coupling coefficient between I_{loop2} and I_{pe}; α and β are always positive. In Type I, which is the case of the single-mode parasitic element, I_{loop1} provides a positive coupling to I_{pe} while I_{loop2} provides a negative coupling to I_{pe}, so I_{pe} can be written as

$$I_{pe} = \alpha I_{loop1} - \beta I_{loop2} \quad (1)$$

From the equation, if we want to avoid the negative coupling, β should be equal to zero. Therefore, part of the current path which is parallel to I_{loop2} is removed in Type II. Then, I_{pe} can be written as

$$I_{pe} = \alpha I_{loop1} \quad (2)$$

However, in this case, the physical length of the corresponding parasitic element can be 5 mm at the maximum because of the thickness limit of smartphones; it is too short for the parasitic element to resonate in 5 GHz band. Thus, we need to create a new current path for the parasitic element to extend its electrical length; besides, the new path should be able to avoid the negative coupling and even obtain more positive coupling from I_{loop1} and I_{loop2}. One effective solution is shown in Type III. From the current distribution in Type III, it can be seen that although I_{loop1} and I_{loop2} are anti-phase, they both provide positive coupling to the new current path. As a result, I_{pe} can be written as

$$I_{pe} = \alpha I_{loop1} + \beta I_{loop2} \quad (3)$$

By removing part of the old current path and creating a new current path, the minus in equation (1) has been successfully converted into a plus in equation (3); this means more efficient excitation for the parasitic element mode. The next step is to realize the current path of Type III in actual antenna structure.

Based on the loop antenna in Fig. 1, two grounding strips are placed near the feeding point as shown in Fig. 6(b). Strip 2 itself is corresponding to the current path I_{pe} in Type II, but it is too short to resonate in 5GHz band (it should resonate at around 15 GHz as a monopole parasitic element), so strip 1 together with the ground is used to create a dipole current path for strip 2; this dipole current path is corresponding to the current path I_{pe} in Type III. In other words, section BCDEF is a dipole parasitic element. Besides, it is easy to find that section BCD can also operate as a monopole parasitic element. As a result, the proposed parasitic element can operate at a monopole-like 0.25λ mode and a dipole-like 0.5λ mode simultaneously.

As discussed above, the resonant frequency of monopole-like 0.25λ mode is determined by the length of section BCD, while the resonant frequency of dipole-like 0.5λ mode is determined by the length of section BCDEF. Therefore, these two modes can be tuned separately. In this design, the monopole-like 0.25λ mode is used to cover 3400-3800 MHz for LTE bands 42/43, and the dipole-like 0.5λ mode in conjunction with other higher order modes of the loop antenna is used to cover 5150-5850MHz for LTE-U/LTE-LAA as shown in Fig. 6(c). From Fig. 6(c), it is also noticeable that the proposed monopole/dipole parasitic element has little effect on the main loop antenna modes, which makes it easy to design.

C. Radiation Mechanisms

In order to further demonstrate the principle of the proposed antenna, surface current distributions and 3-D radiation patterns of six resonant modes are simulated and shown in Fig. 7 and Fig. 8 respectively. From the S11 in Fig. 6(c), it can be easily seen that 0.5λ, 1λ, 1.5λ, 2λ, monopole-like 0.25λ, and dipole-like 0.5λ modes resonate at around 920 MHz, 1745 MHz, 2085 MHz, 2560 MHz, 3640 MHz, and 5345 MHz respectively. Therefore, these frequency points are chosen for the demonstration.

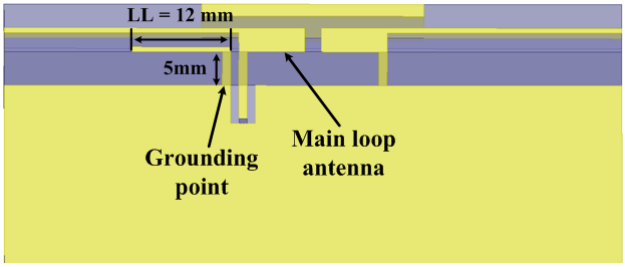

(a)

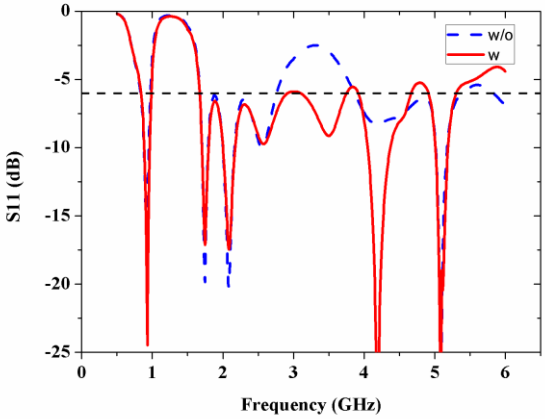

(b)

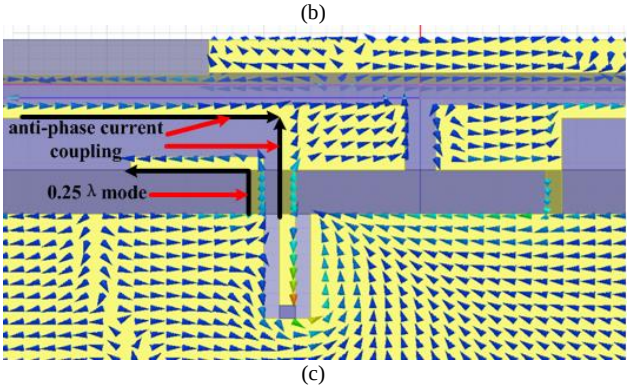

(c)

Fig. 5. (a) Configuration of single-mode parasitic element. (b) Comparison of S11 between loop antennas with and without single-mode parasitic element. (c) Vector current distribution at 5.5 GHz when LL = 8.5 mm.

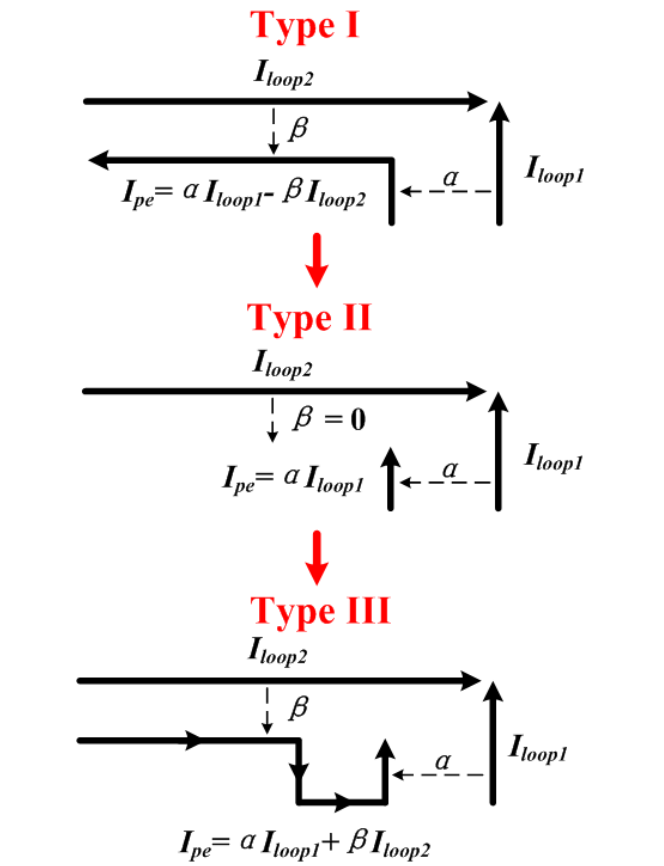

(a)

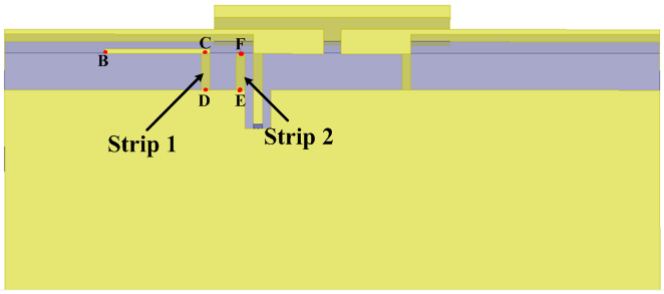

(b)

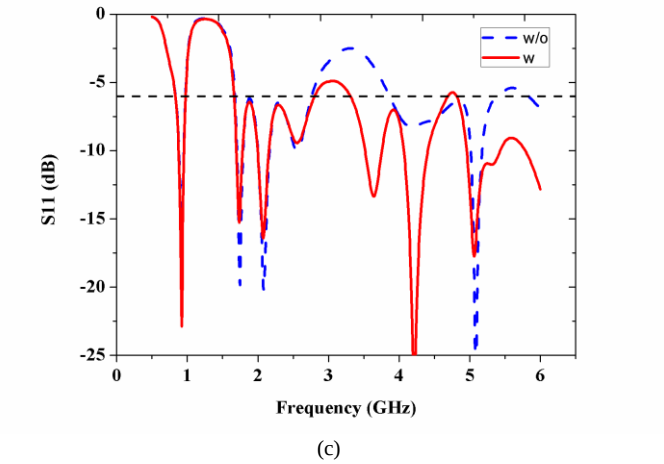

(c)

Fig. 6. (a) Current path model for the evolution of parasitic element technology. (b) Configuration of monopole/dipole parasitic element. BC = 12, CD = 5, DE = 4 and FE = 5 mm. (c) Comparison of S11 between loop antennas with and without monopole/dipole parasitic element.

From vector surface current distributions in Fig. 7(a)-(d), it is clearly shown that there are one, two, three, and four current nulls on loop antenna track respectively. This proves that these four modes are 0.5λ, 1λ, 1.5λ, and 2λ modes respectively. From vector surface current distribution in Fig. 7(e), it can be observed that there is strong current on strip 1, and only one current null exists at the open end of strip 1 together with one current maximum at the grounding point of strip 1, so this mode is monopole-like 0.25λ mode that is an unbalanced mode. Besides, there is little energy on strip 2 in this case, so strip 2 does not work at this mode. From vector surface current distribution in Fig. 7(f), it is easy to find that there is strong current along the path from strip 1 to strip 2, and there are one current null at the open end of strip 1, another current null at the open end of strip 2, and one current maximum in the middle of the path. As a result, this mode is dipole-like 0.5λ mode, which is a balanced mode.

Balanced modes are superior to unbalanced modes because there is much less current density distribution on PCB, which benefits user interaction robustness. From the surface current density distributions in Fig. 7(a)-(f), it can be clearly seen that for the current distribution on PCB, the energy of 1λ, 2λ, and dipole-like 0.5λ modes is much weaker than the energy of 0.5λ, 1.5λ, and monopole-like 0.25λ modes. This phenomenon also demonstrates that the firstly introduced dipole-like 0.5λ mode for parasitic element is a balanced mode from another point of view.

From the 3-D radiation patterns shown in Fig. 8(a)-(d), it can be observed that these four 3-D patterns are typical patterns of loop antenna 0.5λ, 1λ, 1.5λ, and 2λ modes respectively. The pattern in Fig. 8(e) has more nulls than the patterns in Fig. 8(a)-(d), because the radiator of this mode, which consists of strip 1 and PCB, has much larger electrical size. It can be also seen that most of electromagnetic field energy radiates towards +y direction. It is because the radiated energy from the source current of strip 1 and the induced current on PCB will in-phase stack, but PCB only exists in +y direction, so the induced current only exists in +y direction but not in –y direction, and thus the phenomenon of in-phase stacking only happens in +y direction but not in –y direction. From Fig. 8(f), it can be found that most of the energy radiates along y-axis. The reason is that the main radiation source of this mode is strip 1 and strip 2, so the current concentrates on these two strips, which means the current direction is along either x-axis or z-axis and the current in both directions has the strongest radiation in y direction.

D. Design Guidance

Generally, the design of multimode antennas is complicated because designers need to take into account all the operating modes simultaneously. In order to simplify the design complexity of the proposed six-mode antenna, some design principles are given below:

(1) The six-mode design can be divided into two parts, i.e. the design of the four loop antennas modes and the design of the two parasitic element modes. As shown in Fig. 6(c), the parasitic element modes have little effect on the operating state of the loop antenna modes. As a result, designers can design the

main loop antenna first and add the monopole/dipole parasitic element afterwards. Four-mode design and two-mode design should be much easier than six-mode design.

(2) For the loop antenna design, the initial length of the loop antenna should be set as half-wavelength at 900 MHz. That is

$$2 \times (2 \times H + L1 + L2 + L3) + L = \lambda_1/2 \quad (4)$$

$$\lambda_1 = c/f_1 \quad (5)$$

where c is the speed of light in vacuum and f_1 is the frequency value of 900 MHz. Then, the widened portion A should be added and maintained during the whole tuning process. Afterwards, utilize reactive loading (in the proposed antenna, it is the widened portion with the width of H+$L5$) to tune the resonant frequency of 0.5λ, 1λ, 1.5λ, and 2λ modes to proper position. Finally, a highpass matching circuit should be used to expand the bandwidth of 0.5λ mode.

(3) For the design of the monopole/dipole parasitic element, the initial length of the monopole path and the dipole path should be set as quarter-wavelength at 3600 MHz and half-wavelength at 5500 MHz respectively. That is

$$BC + CD = \lambda_2/4 \quad (6)$$

$$BC + CD + DE + EF = \lambda_3/2 \quad (7)$$

$$\lambda_2 = c/f_2 \quad (8)$$

$$\lambda_3 = c/f_3 \quad (9)$$

where f_2 is the frequency value of 3600 MHz and f_3 is the frequency value of 5500 MHz. However, the resonant frequency of the monopole-like 0.25λ mode and the dipole-like 0.5λ mode may deviate from 3600 MHz and 5500 MHz due to the complex electromagnetic coupling environment. Further fine tuning is needed.

III. Measured Results and Discussions

The proposed antenna has been fabricated and measured, and the prototype is shown in Fig. 9(a). As shown in Fig. 9(b), a highpass network, which consists of one shunt inductor (L = 18 nH) and one series capacitor (C = 3 pF), is adopted to enhance the bandwidth of 0.5λ mode and have little influence on the frequency bands above 1.5 GHz. The simulated S11 of the antenna with the matching circuit is shown in Fig. 9(c). From the measured S11 in Fig. 9(c), it can be seen that the four loop antenna modes and the two proposed parasitic element modes have been successfully excited to cover the bands of 660-1100 MHz, 1710-3020 MHz,3370-3900 MHz, and 5150-5850 MHz, which is wide enough for almost all the service of mobile telecommunication systems. In the measured result, the resonant frequency of the six modes is a little higher than the simulated result because of the rough handmade prototype. However, it still indicates good agreement between the measured and simulated results.

The simulated and measured radiation efficiency is shown in Fig. 10. In the bands of 690-1100 MHz and 1710-3020 MHz, the frequency of peak points in the measured efficiency is also higher than that in the simulated efficiency because of the fabrication error. In the band of 3370-3900 MHz, the measured result shows excellent agreement with the simulated result. In the band of 5150-5850 MHz, the measured curve is a little different from the simulated curve because the electrical characteristics is much more sensitive in such high frequency, which means small dimension error may cause big difference. It should be noticed that the measured efficiency at around 2.7 GHz and 5.27 GHz is higher than the simulated result. The reason is that at 2.7 GHz and 5.27 GHz, the measured S11 (shown in Fig. 9(c)) is much better than the simulated S11 so the total radiation percentage of electromagnetic field energy increases a lot. In summary, reasonable agreement is obtained between the measured and simulated results.

The bandwidth of the measured radiation efficiency better than 30% is 704-1100 MHz, 1710-3020 MHz, 3370-3840 MHz and 5150-5850 MHz. If efficiency better than 59% is chosen as the criteria, the bandwidth should be 775-1070 MHz, 1710-3020 MHz, 3370-3840 MHz and 5150-5850 MHz. It should be mentioned that in practical applications, the 0.5λ mode of the loop antenna can be tuned to lower resonant frequency to achieve better efficiency in the band of 698-960 MHz.

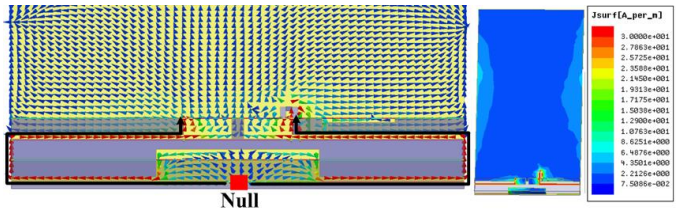

(a)

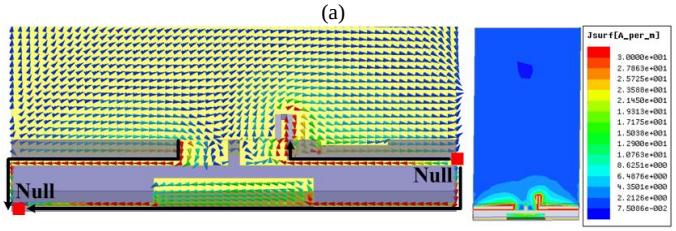

(b)

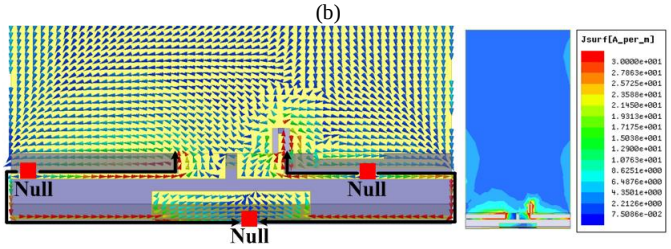

(c)

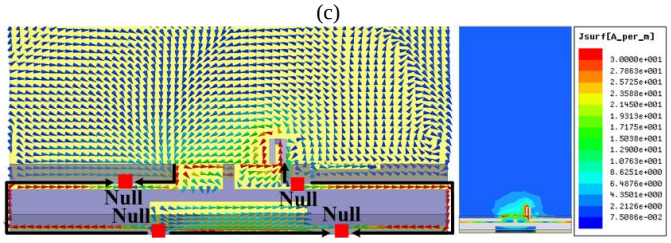

(d)

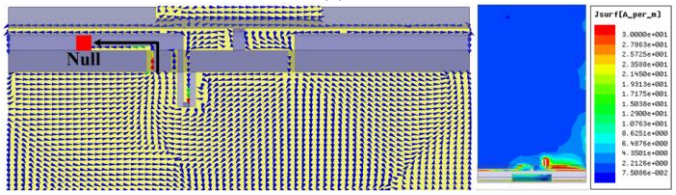

(e)

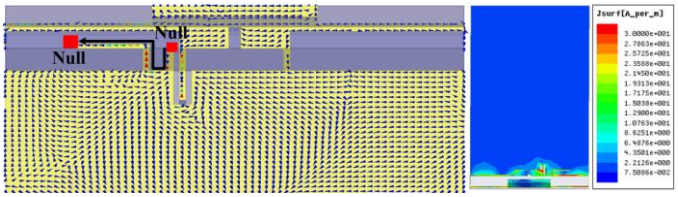

(f)

Fig. 7. Vector surface current distributions and current density distributions at (a) f = 920 MHz. (b) f = 1745 MHz. (c) f = 2085 MHz. (d) f = 2560 MHz. (e) f = 3640 MHz. (f) f = 5345 MHz.

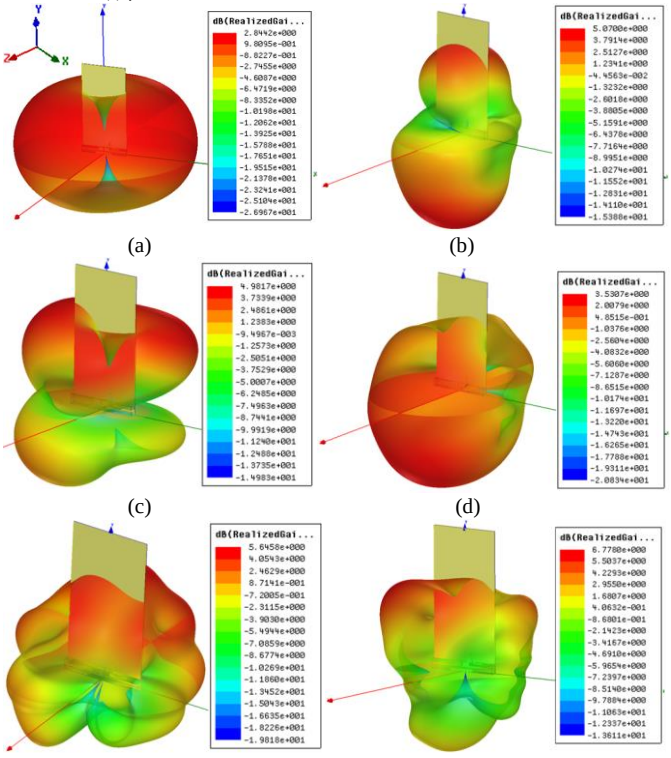

(a) (b) (c) (d) (e) (f)

Fig. 8.Simulated 3-D radiation patterns at (a) f = 920 MHz. (b) f = 1745 MHz. (c) f = 2085 MHz. (d) f = 2560 MHz. (e) f = 3640 MHz. (f) f = 5345 MHz.

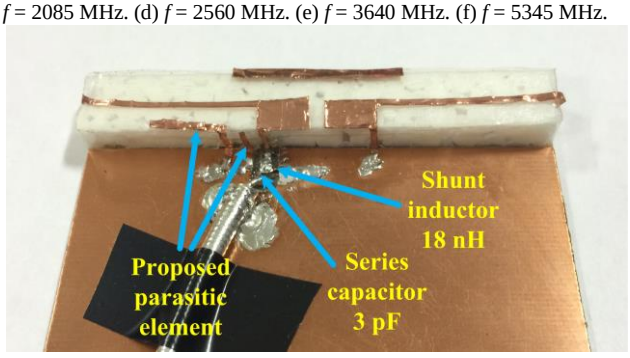

(a)

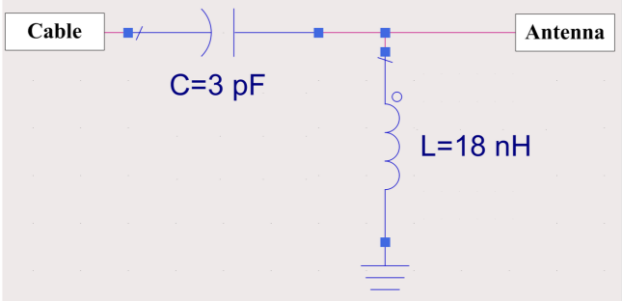

(b)

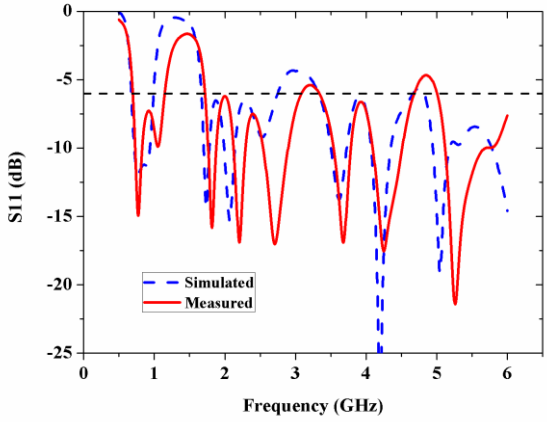

(c)

Fig. 9.(a) Fabricated antenna. (b) Highpass matching circuit. (c) Simulated and measured S11 of proposed antenna.

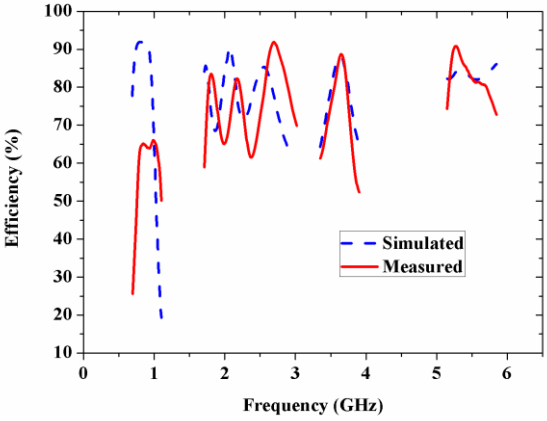

Fig. 10. Simulated and measured radiation efficiency.

IV. Conclusion

A novel multiband loop antenna with six resonant modes has been proposed for LTE smartphones. The distinctive feature of the proposed antenna is that the proposed monopole/dipole parasitic element offers one extra monopole-like 0.25λ mode and one extra balanced dipole-like 0.5λ mode, which together with four loop antenna modes can be utilized to cover the bands of 660-1100 MHz, 1710-3020 MHz, 3370-3900 MHz, and 5150-5850 MHz. These four bands are wide enough for almost all the service of mobile telecommunication systems such as GSM850, GSM900, DCS1800, PCS1900, UMTS, 2.4GHz Wi-Fi, FDD-LTE bands(1-10, 12-14, 17-20, 22, 23, 25-31), TDD-LTE bands (33-44), and even the coming LTE-U/LTE-LAA. Bandwidth comparison between our proposed loop antenna and the loop antennas in the latest published papers is shown in TABLE I. It can be clearly seen that the proposed antenna has the widest bandwidth in an acceptable clearance area.

Another advantage of the proposed antenna is the extra balanced mode, i.e. dipole-like 0.5λ mode of the parasitic element. It should be the first time to report a balanced mode for a parasitic element. Furthermore, the proposed antenna

should be the first loop antenna which has three balanced modes. As is known, balanced modes have better user interaction robustness and smaller specific absorption rate (SAR) than unbalanced modes. This enables the proposed antenna to provide better user experience. It is also worth mentioning that the proposed monopole/dipole parasitic element does not need any additional space for loop antennas and has little effect on the main loop antenna modes. This makes the parasitic element easy to design and tune in practical applications. Some design principles have been given in this paper.

Overall, the proposed antenna has solved the problem of excellent user experience but limited bandwidth in loop antennas. It is a promising candidate for LTE smartphone application.

TABLE I
BANDWIDTH COMPARISON

Ref.	Proposed	[4]	[5]	[7]	[8]
Clearance area (mm^2)	75×10	50×13	68×3	60×8	70×10 +70×5
-6 dB bandwidth (MHz)	660-1100 1710-3020 3370-3900 5150-5850	698-960 1710-2300 — —	780-1020 1650-2120 — —	800-1100 1700-2580 — —	770-1130 1612-3000 — —
>59% efficiency bandwidth (MHz)	775-1070 1710-3020 3370-3840 5150-5850	720-960 1710-2300 — —	820-1000 — — —	830-1140 1680-2570 — —	824-960 1710-2690 — —

ACKNOWLEDGMENT

Many thanks to Simon Jakes at the University of Kent for the antenna fabrication. Also many thanks to Sabrina Ariffin at the University of Kent for her help in English Writing.

REFERENCES

[1] Y.W. Chi, and K.L. Wong, "Compact Multiband Folded Loop Chip Antenna for Small-Size Mobile Phone," *IEEE Trans. Antennas Propag.*, vol. 56, no. 12, pp. 3797-3803, Dec. 2008.

[2] K.L. Wong and C.H. Huang, "Printed Loop Antenna With a Perpendicular Feed for Penta-Band Mobile Phone Application," *IEEE Trans. Antennas Propag.*, vol. 56, no. 7, pp. 2138-2141, Jul. 2008.

[3] H.F. Abutarboush, et al, "Multiband Inverted-F Antenna With Independent Bands for Small and Slim Cellular Mobile Handsets," *IEEE Trans. Antennas Propag.*, vol. 59, no. 7, pp. 2636-2645, Jul. 2011.

[4] M. Zheng, et al, "Internal Hexa-band Folded Monopole/Dipole/Loop Antenna With Four Resonances for Mobile Device," *IEEE Trans. Antennas Propag.*, vol. 60, no. 6, pp. 2880–2885, Jun. 2012.

[5] K. Ishimiya, C.Y. Chiu and J.I. Takada, "Multiband Loop Handset Antenna With Less Ground Clearance," *IEEE Antennas Wireless Propag. Lett.*, vol. 12, pp. 1444-1447, 2013.

[6] K.L. Wong and M.T. Chen, "Small-Size LTE/WWAN Printed Loop Antenna With an Inductively Coupled Branch Strip for Bandwidth Enhancement in The Tablet Computer," *IEEE Trans. Antennas Propag.*, vol. 61, no. 12, pp. 6144-6151, Dec. 2013.

[7] D. Wu, S.W. Cheung, and T.I. Yuk, "A Compact and Low-Profile Loop Antenna With Multiband Operation for Ultra-Thin Smartphones," *IEEE Trans. Antennas Propag.*, vol. 63, no. 6, pp. 2745-2750, Jun. 2015.

[8] Y.L. Ban, et al, "A Dual-Loop Antenna Design for Hepta-Band WWAN/LTE Metal-Rimmed Smartphone Applications," *IEEE Trans. Antennas Propag.*, vol. 63, no. 1, pp. 48-58, Jan. 2015.

[9] M. Zheng, "A Multi-Band Antenna," US patent 7,307,591 B2, Jul. 20, 2004.

[10] H. Y. Wang, M. Zheng, and S. Brett, "A Multi-Band Antenna," US patent 7,205,942 B2, Jul. 6, 2005.

[11] Y. Li, Z.J. Zhang, J.F. Zheng, Z.H. Feng and M.F. Iskander, "A Compact Hepta-Band Loop-Inverted F Reconfigurable Antenna for Mobile Phone," *IEEE Trans. Antennas Propag.*,vol. 60, no. 1, pp. 389–392, Jan. 2012.

[12] Y. Li, Z.J. Zhang, J.F. Zheng and Z.H. Feng, "Compact Heptaband Reconfigurable Loop Antenna for Mobile Handset," *IEEE Antennas Wireless Propag. Lett.*, vol. 10, pp. 1162-1165, 2011.

[13] H. T. Chen, K. L. Wong, and T. W. Chiou, "PIFA With a Meandered and Folded Patch for the Dual-Band Mobile Phone Application," *IEEE Trans. Antennas Propag.*,vol. 51, no. 9, pp. 2468–2471, Sep. 2003.

[14] H. Y. Wang, and M. Zheng, "An Internal Triple-Band WLAN Antenna," *IEEE Antennas Wireless Propag. Lett.*, vol. 10, pp. 569-572, 2011.

[15] K. L. Wong, W. Y. Chen and T. W. Kang, "On-Board Printed Coupled-Fed Loop Antenna in Close Proximity to the Surrounding Ground Plane for Penta-Band WWAN Mobile Phone," *IEEE Trans. Antennas Propag.*,vol. 59, no. 3, pp. 751–757, Mar. 2011.

[16] Y. L. Ban, C. L. Liu, J. L. W. Li, J. H. Guo and Y. J. Kang, "Small-Size Coupled-Fed Antenna With Two Printed Distributed Inductors for Seven-Band WWAN/LTE Mobile Handset," *IEEE Trans. Antennas Propag.*, vol. 61, no. 11, pp. 5780–5784, Nov. 2013.

[17] L. Li, et al, "A Novel Compact Multiband Antenna Employing Dual-Band CRLH-TL for Smart Mobile Phone Application," *IEEE Antennas Wireless Propag. Lett.*, vol. 12, pp. 1688-1691, 2013.

[18] H. Liu, et al., "Novel Miniaturized Octaband Antenna for LTE Smart Handset Applications," *International Journal of Antennas and Propagation*, Volume 2015, Article ID 861016, 8 pages, 2015

[19] Y. W. Chi and K. L. Wong, "Internal compact dual-band printed loop antenna for mobile phone application," *IEEE Trans. Antennas Propag.*, vol. 55, no. 5, pp. 1457–1462, May 2007.

[20] C. I. Lin and K.L. Wong, "Internal meandered loop antenna for GSM/DCS/PCS multiband operation in a mobile phone with the user's hand," *Microw. Opt. Technol. Lett.*, vol. 49, pp. 759–766, Apr. 2007.

[21] H. Morishita, et al, "Performance of balance-fed antenna system for handsets in the vicinity of a human head or hand," *Proc. Inst. Elect. Eng. Microw. Antennas Propag.*, vol. 149, pp. 85–91, Apr. 2002.

[22] Qualcomm, "Making the best use of licensed and unlicensed spectrum," https://www.qualcomm.com/media/documents/files/making-the-best-use-of-unlicensed-spectrum-presentation.pdf, September 2015.

[23] R. Zhang, et al, "LTE-Unlicensed: The Future of Spectrum Aggregation for Cellular Networks," *IEEE Wireless Communications*, vol. 22, no. 3, pp. 150-159, Jun. 2015.

[24] Ansoft Corporation HFSS [Online]. Available: http://www.ansoft.com/products/hf/hfss/

[25] Testing and Measurement Techniques-Reverberation Chamber Test Methods, IEC 61000-4-21, 2011.

[26] C.L. Hooloway, et al, "Reverberation Chamber Techniques for Determining the Radiation and Total Efficiency of Antennas," *IEEE Trans. Antennas Propag.*, vol.60, no. 4, pp. 1758-1770, Apr. 2012.

[27] Q. Xu, et al, "A Modified Two-antenna Method to Measure the Radiation Efficiency of Antennas in a Reverberation Chamber," *IEEE Antennas Wireless Propag. Lett.*, vol. 15, pp. 336-339, 2016.

[28] H. Y. Wang and M. Zheng, "Triple-band wireless local area networkmonopole antenna," *IET Microw. Antennas Propag.*, vol. 2, no.4, pp. 367–372, May 2008.

[29] P. Vainikainen, et al, "Resonator-Based Analysis of the Combination of Mobile Handset Antenna and Chassis," *IEEE Trans. Antennas Propag.*, vol. 50, no. 10, pp. 1433–1444, Oct. 2002.

Hang Xu received his B.S. and M.S. degrees from the University of Electronic Science and Technology of China, Chengdu, China, in 2009 and 2013 respectively. He is currently pursuing the Ph.D. degree at University of Kent, Canterbury, United Kingdom.

His research interests include 5G smartphone antennas, MIMO antenna arrays, decoupling technology, microwave and millimeter-wave antennas.

Hanyang Wang (SM'03) received the Ph.D. degree in 1995 from Heriot-Watt University, Edinburgh, UK.

From 1986 to 1991, he served as a lecturer and associate professor at Shandong University, Jinan, China. From 1995 to 1999, he was a post-doctoral research fellow at the University of Birmingham and the University of Essex, UK. From 1999 to 2000, he was with Vector Fields Ltd, Oxford, UK, as a software development and microwave engineering consultant engineer. He joined Nokia UK Limited in 2001 and worked at Nokia for 11 years as a mobile antenna specialist. He joined Huawei after leaving Nokia, and he is now the head of the mobile antenna technology division at Huawei Technologies. He is also an adjunct professor at the School of Electronics and Information Technology, Sichuan University, China. His research interests include small antennas for mobile terminals, patch and slotted waveguide antennas and arrays for mobile communications and airborne radars, and numerical methods for the solutions of electromagnetic radiation and scattering problems. He holds over 20 granted and pending US and EU patents, and he is the author of over 60 referred papers on these topics.

Dr. Wang was awarded the title of Nokia Inventor of the Year in 2005 and Nokia Excellence Award in 2011. He was awarded the Huawei Individual Gold Medal Award in 2012 and Huawei Team Gold Medal Award in 2013 and 2014 respectively. He is listed in US Marquis Who's Who in the World and UK IBC (International Biographical Centre, Cambridge, England). He is a Senior Member of IEEE, Fellow of IET/IEE, and Associate Editor of IEEE Antennas and Wireless Propagation Letters.

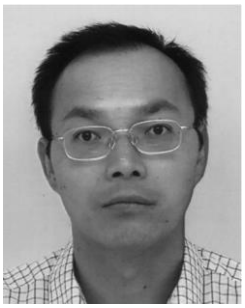

Steven Gao (M'01) received the Ph.D. degree in Microwave Engineering from Shanghai University, Shanghai, China.

He is a Professor and Chair of RF and Microwave Engineering with the University of Kent, Canterbury, U.K. He started his career since 1994 while at China Research Institute of Radiowave Propagation. Afterward, he worked as a Post-doctoral Research Fellow with the National University of Singapore, Singapore, a Research Fellow with Birmingham University, Birmingham, U.K., a Visiting Research Scientist at Swiss Federal Institute of Technology (ETHZ), Zürich, Switzerland, a Visiting Fellow at Chiba University (Japan), a Visiting Scientist at the University of California at Santa Barbara, Santa Barbara, USA, a Senior Lecturer, Reader, and Head of Antenna and Microwave Group with Northumbria University, Newcastle upon Tyne, U.K., and the Head of Satellite Antennas and RF System Group with Surrey Space Centre, University of Surrey, Surrey, U.K. He is a Professor with the University of Kent, since January 2013. He is an IEEE AP-S Distinguished Lecturer, an Associate Editor of IEEE Trans. on Antennas and Propagation, an Associate Editor of Radio Science, and Editor-in-Chief for Wiley Book Series on "Microwave and Wireless Technologies." He co-edited Space Antenna Handbook (Wiley, 2012) and co-authored Circularly Polarized Antennas (IEEE-Wiley, 2014), over 250 papers and several patents. His research interests include smart antennas, phased arrays, MIMO, satellite antennas, microwave/mm-wave/THz circuits, satellite and mobile communications, and radar (UWB radar, synthetic-aperture radar) and wireless power transfer.

Dr. Gao is a Fellow of IET, U.K, was General Chair of LAPC 2013, and an Invited or Keynote Speaker of some international conferences such as AES'2014, IWAT'2014, SOMIRES'2013, and APCAP'2014 .

Hai Zhou received a Ph.D degree on reflector antenna synthesis in 1987 from University of London, where he also carried out his post doctoral work until 1992. He served as a senior lecturer at South Bank University, London before joining Lucent Technologies in 1996, working on GSM, UMTS and LTE in system engineering before joining Huawei Technologies in 2015.

He worked on various topics from shaped reflector antenna synthesis, FDTD during his academic years to radio resource management and adaptive antennas in industry, with 18 patents, 14 journal papers and 34 conference papers. One of the papers won the Best Paper Award at the 19th European Microwave Conference in 1989, another received Oliver Lodge premium from IEE as the best paper of the year on Antennas and Propagation in 1991.

Yi Huang (SM'06) is a Professor with the University of Liverpool, Liverpool, U.K..

Qian Xu received the Ph.D. degree at University of Liverpool, Liverpool, U.K., in 2016.

He is currently a lecturer with the Nanjing University of Aeronautics and Astronautics, Nanjing, China.

Yujian Cheng (SM'14) is a Professor with the University of Electronic Science and Technology of China, Chengdu, China.